Available online at www.sciencedirect.com
SCIENCE DIRECT®

Journal of Organometallic Chemistry 666 (2003) 23–34

ELSEVIER

Journal of Organometallic Chemistry

www.elsevier.com/locate/jorganchem

Group 13 trihalide complexes of 9-fluorenone: a comparison of methods for assigning relative Lewis acidity

Catherine S. Branch [a], Simon G. Bott [b,*], Andrew R. Barron [a,*]

[a] *Department of Chemistry and Center for Nanoscale Science and Technology, Rice University, 6100 Main Street, Houston, TX 77005, USA*
[b] *Department of Chemistry, University of Houston, Houston, TX 77204, USA*

Received 28 June 2002

Dedicated to Jerry L. Atwood who has added so much to our structural knowledge of Group 13 Lewis acid–base complexes, as well as being a true colleague, mentor and friend

---

Abstract

The 9-fluorenone complexes MX_3(9-fluorenone) [M = B, X = Cl (**1**); M = Al, X = Cl, Br (**2**), I (**4**), M = Ga; X = Cl (**5**), Br (**6**), I (**7**) and $AlBr_3$(9-fluorenone)$_2$ (**3**) have been prepared and characterized by NMR, IR and UV–vis spectroscopy and X-ray crystallography (**1**, **2**, **3**, **5** and **6**). Complexes of $MgCl_2$ (**8**), $HgCl_2$ (**9**), $ZrCl_4$ (**10**) and $SnCl_4$ (**11**) were characterized by IR and UV–vis spectroscopy, while the unusual mixed vanadium(IV,V) compound, VO(Cl)(9-fluorenone)$_2$(H_2O)(μ-O)($VOCl_2$) (**12**) has been structurally characterized. Solution ligand dissociation energies for MX_3(9-fluorenone) were determined by variable temperature ^{1}H-NMR spectroscopy. For all the compounds, ΔS_D is large and positive, as would be expected from a dissociative process. A correlation of the results for the five structurally characterized compounds MX_3(9-fluorenone) (M = B, X = Cl; M = Al, X = Cl, Br; M = Ga, X = Cl, Br) was used to examine the suitability of the following parameters to measuring Lewis acidity: IR $\nu_{C=O}$, UV λ_{max}, and ^{13}C-NMR $\delta_{C=O}$, K_{eq} at 298 K, ΔH, ΔG, and a variety of structural parameters. Parameters determined from X-ray crystallography appear to be controlled by inter-ligand repulsion or the ionic radii of the metal atom. The change in the $\nu_{C=O}$ band upon coordination provides a reasonable ordering for a specific metal (i.e. $AlI_3 \approx AlBr_3 > AlCl_3$), but does differentiate simply between 1:1 and 1:2 complexes. Unexplainably, the shift in the $\delta_{C=O}$ in the ^{13}C-NMR appears to be the complete opposite of other trends. It appears important to differentiate, the ability of a Lewis acidic compound to bind a Lewis base from the effect the metal compound has upon that Lewis base once coordinated. In this regard, the K_{eq} at 298 K and ΔG would appear to be the best measures of the ability of a Lewis acid to bind a specific Lewis base, while the $\Delta\lambda_{max}$ for the 9- fluorenone complexes provides a good indication as to the effect of a Lewis acid on a particular Lewis base.

Keywords: Trihalide complexes; 9-Fluorenone; Lewis acidity; Aluminium; Gallium

---

1. Introduction

Forty years ago Lappert noted that the one drawback with Lewis' theory of acids and bases is its failure to 'come to terms with quantitative aspects' [1]. Despite attempts by many researchers there is still no clear quantitative measure of Lewis acidity. The measurement the strength of a Lewis base is actually more refined. Tolman developed a simple approach for the measurement of the electron donor ability properties of phosphorous ligands towards transition metals [2], which in combination with his concepts of cone angle [3] may be used to predict relative reactivity and structures of Lewis acid–base complexes including those for main group metals [4].

The strength of Brønsted acid–base interactions has been thoroughly explored, but quantifying the strengths of Lewis acid–base interactions has proven much more difficult [5]. Olah et al. have suggested that 'strength' has no real meaning for Lewis acids [6]. Nevertheless, attempts to correlate Lewis acid strength with various spectroscopic data have been successful. The closest to a

---

* Corresponding authors. Tel.: +1-713-3485610; fax: +1-713-3485203; url: www.rice.edu/barron
E-mail address: arb@rice.edu (A.R. Barron).

PII: S0022-328X(02)02029-6

method for the actual value of Lewis acidity involves the calculation or measurement of the enthalpy change accompanying the formation of a Lewis acid–base complex in the absence of solvation effects, i.e. the bond dissociation energy (BDE) in the vapor phase. However, this method is not readily available for a wide range of compounds and so an alternative, more experimentally accessible, approach is required. The strength of the M–L bond in $MX_3R_{3-n}(L)$ complexes has been studied in solution using NMR spectroscopy [7–10]. Additionally, bond lengths as determined by X-ray diffraction have yielded sequences of Lewis acidity [11]. Interestingly, more precise measurement of Lewis acidity in solid systems has been attempted due to the importance of Lewis acid cites in heterogeneous catalysis [12,13].

In trying to define a simple qualitative scale for Lewis acidity, Lappert suggested the use of IR spectroscopic shifts of the carbonyl stretching frequency for ethyl acetate [1]. Perturbations in the $\nu_{C=O}$ were taken to reflect polarization of the C=O bond and thus the strength of the Lewis acid [14]. Based upon this approach a relative orders for MX_3 was determined to be Br > Cl for B and Al, but Cl > Br for In, and the group trend was determined to be B > Ga > Al > In [1]. Several other studies have developed similar trends [15]. Lazlo and Teston suggested that Lewis acidities be based upon the π* energy level in the 1:1 complex formed between the Lewis acid and crotonaldehyde [16,17]. This also follows a trend similar to that found by Lappert [1]. It should be noted, however, that in these and other studies, a single parameter was employed as a measure of Lewis acidity. In an alternative approach, Carlson et al. suggested that the selection of Lewis acid catalysts for various organic reactions could be accomplished by a principle component analysis of measured Lewis acid properties [18]. While this computer-assisted strategy showed promise, the descriptors employed were not properties of a Lewis acid–base complex, but the uncomplexed Lewis acid (e.g. dielectric constant, ionization potential, and magnetic susceptibility). As part of our long-standing interest in understanding Lewis acid–base interactions for the Group 13 metals, we have investigated a range of possible alternative parameters that may be used in determining the relative Lewis acidity for Group 13 compounds.

We have previously measured solution BDEs using variable temperature NMR spectroscopy [10a]. Solution measurements do not take into account different solvation effects for reactants and products; however, they have been used as comparative values. Given that the applications of Lewis acids as catalysts and reagents is predominantly in solution, these are actually more relevant than vapor phase measurements and as such are appropriate values to consider. We have previously shown that in addition to the $\nu_{C=O}$ for organic carbonyls, the ^{13}C-NMR shift of the α-carbon is affected by coordination to a Lewis acid [19]. Thus, these parameters were also considered. In line with work of Lazlo and Teston, we have shown that the reduction potential of a ketone is affected by complexation to a Lewis acid [19]. We have therefore investigated the UV spectroscopy as a measure of the relative π* energy level. Finally, X-ray crystallographic data has been used as an estimate of the strength of M–O bonds interactions in alkoxides [20], and the relative Lewis acidity of a metal moiety. The comparison of structural data for a homologous series of $MX_3(L)$ complexes will be investigated.

In choosing a $MX_3(L)$ system for study, both the Lewis base (L) and ancillary ligands (X) must allow characterization by the methods described above. Based on Lappert's and our prior work [1,19], an organic carbonyl is desirable to allow for IR measurements. Furthermore, the particular organic carbonyl must allow for ease of NMR characterization, promote crystallization, and provide a suitable absorption in the UV–vis. In order to limit any potential reactivity (e.g. reduction or alkylation) and obviate issues of complex formulation (e.g. the 1:2 complexes commonly formed with InX_3) we have limited the present study to the tri-halides MX_3, where M = B, Al, Ga and X = Cl, Br, I. There have been extensive studies of the organic carbonyl complexes of aluminum trihalides and to a lesser extent the other Group 13 metals [21–25]. Of the wide range of possible ligands, 9-fluorenone (**I**) offers a potential as a suitable ligand [26], and the complex $AlCl_3$(9-fluorenone) has previously been characterized by X-ray crystallography [25].

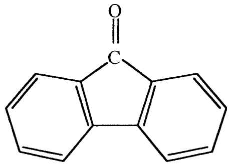

(**I**)

2. Results and discussion

2.1. Characterization of 9-fluorenone complexes

The Lewis acid–base complexes MX_3(9-fluorenone) (M = B, Al, Ga; X = Cl, Br, I) were prepared in toluene solution and isolated as orange to red crystalline solids, where M = B; X = Cl (**1**), M = Al; X = Cl [25], Br (**2**), I (**4**), M = Ga; X = Cl (**5**), Br (**6**), I (**7**) (see Section 3). During the synthesis of the aluminum tribromide complex, two different colored crystals were observed. In addition to the dark red product, $AlBr_3$(9-fluorenone) (**2**), a small quantity (< 10%) of light red crystals was isolated. These were determined to be due to the bis-9-fluorenone complex, $AlBr_3$(9-fluorenone)$_2$ (**3**). A mixture of compounds **2** and **3** were isolated irrespective of the Al–9-fluorenone ratio of the reaction mixture. No bis-9-fluorenone complexes were isolated for the other metal or halide combinations.

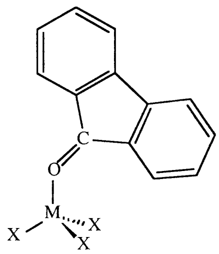

M = B; X = Cl (**1**), M = Al; X= Br (**2**), I (**4**), M = Ga; X = Cl (**5**), Br (**6**), I (**7**)

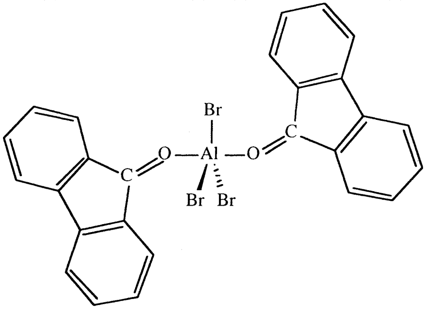

(**3**)

Compounds **1**–**7** were characterized by IR, NMR and UV–vis spectroscopy (see Table 1 and Section 3). In addition, the molecular structures of compounds **1**, **2**, **5** and **6** have been confirmed by X-ray crystallography.

We have previously demonstrated that the complexation of ketones to an aluminum Lewis acid results in an increase of the contribution of resonance form **II** over **III**, resulting in a decrease in the C=O bond order and placing a positive charge on the α-carbon.

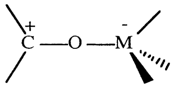

(**II**)

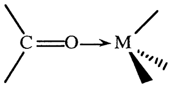

(**III**)

The reduction of the C=O bond strength may be seen from the shift in the IR ($\Delta\nu = 50–130$ cm^{-1}) [21]. A similar effect is observed for MX_3(9-fluorenone) consistent with a weakening of the C=O bond (see Table 1). Furthermore, the $\nu_{C=O}$ stretch for $AlBr_3$(9-fluorenone)$_2$ (**3**) is significantly higher than in $AlBr_3$(9-fluorenone) (**2**) in agreement with the different C=O bond lengths observed in the solid state (see below). IR spectra were also obtained for 9-fluorenone complexes of $MgCl_2$ (**8**), $HgCl_2$ (**9**), $ZrCl_4$ (**10**) and $SnCl_4$ (**11**), see Table 1. If the solubility of the halides was insufficient for reaction in toluene solution (Mg, Hg and Zr) synthesis was carried out in the solid state, see Section 3.

We have shown that the effective increase in positive charge on the α-carbon of ketones, upon coordination to Lewis acids, is seen by a downfield shift of the resonance in the ^{13}C-NMR spectrum ($\Delta\delta = 5–25$ ppm) [19,21]. A similar effect is observed for MX_3(9-fluorenone), see Table 1. These shifts are consistent with **II** significantly contributing to the overall resonance structure.

The molecular structures of compound **2** is shown in Fig. 1, as an example of the structure type; selected bond lengths and angles for compounds **1**–**3**, **5** and **6**, along with those for the previously reported $AlCl_3$(9-fluorenone) [25], are given in Table 2. As was reported for $AlCl_3$(9-fluorenone) [25], compounds **1**, **2**, **5** and **6** are monomeric in the solid state with no close intermolecular contacts. Compounds **1**, **2**, and **6** crystallize as toluene solvates and the BCl_3 unit in compound **1** has a rotational disorder about the B–O bond (see Section 3).

Table 1
Carbonyl stretching frequencies for MX_n(9-fluorenone)$_{n'}$

Compound	$\nu_{C=O}$ (cm^{-1})	$\Delta\nu$ (cm^{-1}) [a]	^{13}C $\delta_{(C=O)}$ (ppm) [b]	$\Delta\delta$ (ppm) [b,c]	λ_{max} (nm)
BCl_3(9-fluorenone) (**1**)	1603	120	200.2	6.8	383
$AlCl_3$(9-fluorenone)	1637	86	205.2	11.8	376
$AlBr_3$(9-fluorenone) (**2**)	1634	89	205.0	11.6	380
$AlBr_3$(9-fluorenone)$_2$ (**3**)	1668	55	n/a	n/a	n/a
AlI_3(9-fluorenone) (**4**)	1634	89	n/a	n/a	326
$GaCl_3$(9-fluorenone) (**5**)	1635	88	206.2	12.8	365
$GaBr_3$(9-fluorenone) (**6**)	1636	87	205.2	11.8	367
GaI_3(9-fluorenone) (**7**)	1652	71	n/a	n/a	n/a
$MgCl_2$(9-fluorenone)$_n$ (**8**)	1653	70	n/a	n/a	309
$HgCl_2$(9-fluorenone)$_n$ (**9**)	1697	26	n/a	n/a	324
$ZrCl_4$(9-fluorenone)$_n$ (**10**)	1633	90	n/a	n/a	324
$SnCl_4$(9-fluorenone)$_n$ (**11**)	1635	88	n/a	n/a	297

[a] In comparison with free 9-fluorenone (1723 cm^{-1}).

[b] Determined in the presence of excess MX_3 to ensure complete coordination, see text.

[c] In comparison with free 9-fluorenone ($\delta = 193.4$ ppm).

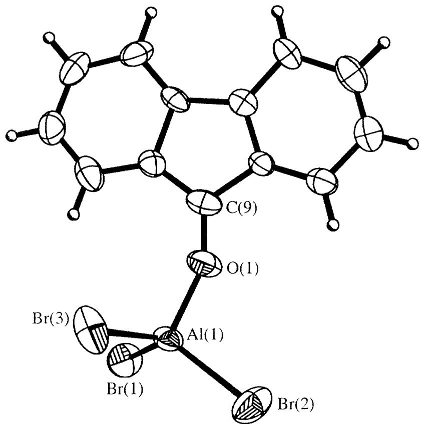

Fig. 1. Molecular structure of $AlBr_3$(9-fluorenone) (**2**). Thermal ellipsoids are shown at the 20% level.

In common with Lewis acid adducts of organic carbonyls, the O=C bond lengths in compounds **1**–**3**, **5** and **6** are increased as compared to the free ligand (Table 2) [27].

The molecular structure of $AlBr_3$(9-fluorenone)$_2$ is shown in Fig. 2; selected bond lengths and angles are given in Table 2. The structure consists of monomeric units, in which the aluminum is five coordinate trigonal bipyramidal with the two 9-fluorenone ligands occupying the axial positions, O(1)–Al(1)–O(1A) angle [174.3(3)°]. The Al and Br atoms lie on a non-crystallographic mirror plane resulting in the 9-fluorenone ligands adopting an eclipsed orientation with each other, but staggered with respect to the equatorial bromides. The orientation of the two 9-fluorenone ligands can also explain the distortions away from an ideal trigonal bipyramidal (see Table 2).

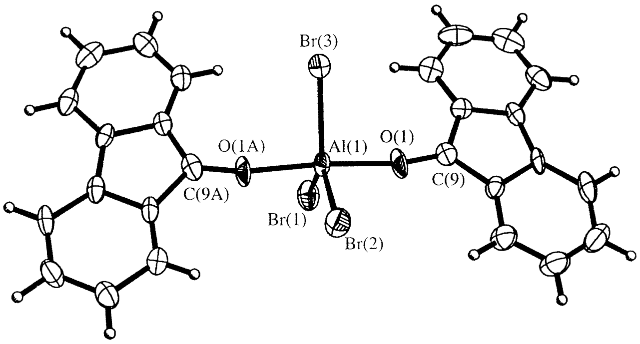

Fig. 2. Molecular structure of $AlBr_3$(9-fluorenone)$_2$ (**3**). Thermal ellipsoids are shown at the 20% level.

During our studies we isolated the unusual mixed vanadium(IV,V) compound, VO(Cl)(9-fluorenone)$_2$(H_2O)(μ-O)($VOCl_2$) (**12**), by reaction of 9-fluorenone with partially hydrolyzed VCl_4. In the presence of water, VCl_4 is rapidly hydrolyzed to give solutions of oxovanadium(IV) chloride. The molecular structure of compound **12** is shown in Fig. 3; selected bond lengths and angles are given in Table 3. The core of the complex is an octahedral vanadium(IV) oxochloride [V(1)] to which is coordinated two 9-fluorenones and a water ligand. The coordination environment of V(1) is completed by a bridging oxo ligand from a $[VO_2Cl_2]^-$ anion. The terminal V=O bond lengths (Table 3) are comparable to those reported for other vanadium oxohalides

Table 2
Selected bond lengths (Å) and angles (°) for MX_3(9-fluorenone)$_n$

M	B	Al	Al	Al	Ga	Ga
X	Cl	Cl	Br	Br	Cl	Br
n	1	1	1	2	1	1
	(1)	[b]	**(2)**	**(3)**	**(5)**	**(6)**
Bond lengths						
M–O	1.514(4)	1.787(3)	1.756(9)	1.907(6), 1.913(7)	1.915(2)	1.936(4)
M–X	1.811(7) [a] 1.833(5) [a] 1.836(4) [a]	2.097(2) 2.109(2) 2.117(2)	2.239(4) 2.253(4) 2.256(4)	2.304(3) 2.312(3) 2.323(3)	2.134(1) 2.125(1) 2.143(1)	2.280(1) 2.288(1) 2.283(1)
O–C	1.261(3)	1.266(5)	1.28(1)	1.25(1), 1.23(1)	1.258(4)	1.258(7)
Bond angles						
O–M–X	108.0(2) [a] 109.5(3) [a] 103.0(2) [a]	105.2(1) 107.2(1) 107.0(1)	102.9(4) 105.7(3) 108.2(3)	88.3(2), 87.4(2) 90.2(2), 89.2(2) 93.7(2), 91.7(2)	101.20(9) 106.79(9) 107.20(9)	101.1(1) 105.2(2) 107.7(1)
X–M–X	112.1(3) 111.8(2) 111.9(3)	110.00(9) 113.18(9) 113.55(9)	112.6(2) 113.1(2) 113.4(2)	114.1(1) 120.6(1) 125.1(1)	114.20(5) 111.21(5) 115.01(5)	113.04(5) 113.22(5) 115.06(5)
O–M–O	n/a	n/a	n/a	174.3(3)	n/a	n/a
M–O–C	135.3(2)	150.2(3)	153(1)	154.4(8), 167.5(7)	143.9(3)	140.7(4)

[a] Major constiuent of rotational disorder.
[b] Ref. [25].

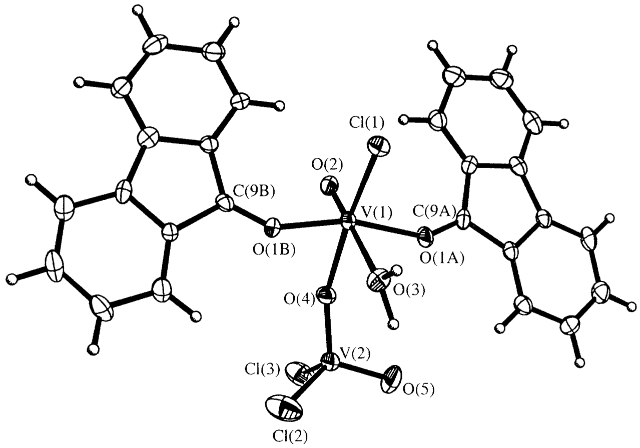

Fig. 3. Molecular structure of $VO(Cl)(9\text{-fluorenone})_2(H_2O)(\mu\text{-}O)(VOCl_2)$ (**12**). Thermal ellipsoids are shown at the 30% level, and hydrogen atoms are omitted for clarity.

(1.55–1.60 Å), and the V–O bonds associated with the 9-fluorenone ligands are within the range expected for V–O single bond interactions (1.91–2.20 Å) [28]. The bridging oxo is asymmetrical, with the V(1)–O(4) and V(2)–O(4) distances consistent with a V–O and V=O bonds, respectively.

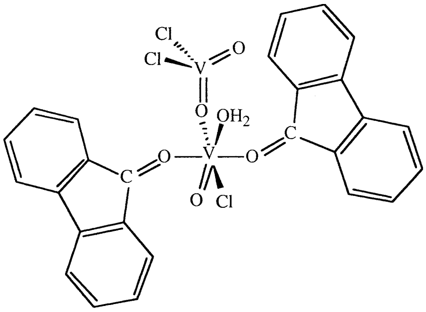

(**12**)

2.2. Solution dissociation energies for MX_3(9-fluorenone)

Given the common occurrence of Lewis acid–base complexes for the Group 13 elements, it is perhaps surprising that reports of thermodynamic data such as BDEs are sparse. The majority of studies have been carried out on the complexes of AlR_3 and AlX_3 ($X = Cl$, Br) [29,30], but recently a wider range of derivatives have been studied [31]. Unfortunately, the dissociation process for the complex is complicated by the dimerization of AlR_3 and thus care must be taken is assigning solution phase measurements as true BDEs [32]. As such we will refer to a 'dissociation energy' rather than a BDE to acknowledge that effects such as solvation and dimerization of the Lewis acid (MX_3) have not been taken into account.

Table 3
Selected bond lengths (Å) and angles (°) in $VO(Cl)(9\text{-fluorenone})_2(H_2O)(\mu\text{-}O)(VOCl_2)$ (**12**)

Bond lengths			
V(1)–O(2)	1.564(4)	V(1)–O(4)	2.014(4)
V(1)–O(1A)	2.013(4)	V(1)–O(1B)	2.031(4)
V(1)–O(3)	2.251(4)	V(1)–Cl(1)	2.336(2)
V(2)–O(5)	1.569(4)	V(2)–O(4)	1.640(4)
V(2)–Cl(2)	2.179(2)	V(2)–Cl(3)	2.187(3)
O(1A)–C(9A)	1.237(6)	O(1B)–C(9B)	1.241(6)
Bond angles			
O(2)–V(1)–O(4)	96.2(2)	O(2)–V(1)–O(1A)	98.3(2)
O(4)–V(1)–O(1A)	87.3(2)	O(2)–V(1)–O(1B)	98.8(2)
O(4)–V(1)–O(1B)	83.1(2)	O(1A)–V(1)–O(1B)	161.2(2)
O(2)–V(1)–O(3)	176.2(2)	O(4)–V(1)–O(3)	80.6(2)
O(1A)–V(1)–O(3)	79.6(2)	O(1B)–V(1)–O(3)	82.9(2)
O(2)–V(1)–Cl(1)	100.8(2)	O(4)–V(1)–Cl(1)	162.7(1)
O(1A)–V(1)–Cl(1)	93.2(1)	O(1B)–V(1)–Cl(1)	91.1(1)
O(3)–V(1)–Cl(1)	82.5(1)	O(5)–V(2)–O(4)	108.8(2)
O(5)–V(2)–Cl(2)	107.9(2)	O(4)–V(2)–Cl(2)	106.9(2)
O(5)–V(2)–Cl(3)	110.2(2)	O(4)–V(2)–Cl(3)	108.8(8)
Cl(2)–V(2)–Cl(3)	114.06(9)	V(2)–O(4)–V(1)	155.6(2)

The relative dissociation energies for such a series of complexes may be derived from the temperature dependence of the equilibrium constant, K_{eq} (Eq. (1)).

$$MX_3(\text{9-fluorenone}) \overset{K_{eq}}{\rightleftharpoons} MX_3 + \text{9-fluorenone} \qquad (1)$$

The ^{1}H-NMR spectrum of 9-fluorenone is not simple due to overlapping peaks, and is described as ABMX. However, upon complexation to MX_3 simplifies the spectrum somewhat. The deshielding of 1-CH proton by the carbonyl group gives rise to a doublet downfield from the remainder of the spectrum, making this a suitable probe for equilibrium measurements. Unfortunately, the ^{1}H-NMR spectra for MX_3(9-fluorenone) show a single doublet arising from the 1-CH protons over the temperature ranges measure, indicating that the equilibria shown in Eq. (1) are rapid on the NMR time scale. In these situations a common method is to derive the K_{eq} assuming the ^{1}H-NMR chemical shift of the 1-CH proton is directly proportional to the mole fraction of the total species present as uncomplexed or 'free' 9-fluorenone. The ^{1}H-NMR for 9-fluorenone has a slight concentration dependence of the ^{1}H-NMR chemical shifts in C_6D_6. Drake and Jones reported a similar dependence using $CDCl_3$ as a solvent [33]. To correct for this effect, all solutions used to determine K_{eq} must have equal concentrations of fluorenone. In addition to a concentration dependence, the ^{1}H-NMR chemical shifts of fluorenone concentration dependent, some temperature dependence was observed. Temperature-corrected shifts were subsequently employed for all calculations.

The enthalpy (ΔH) and entropy (ΔS) were calculated from the associated $\ln(K_{eq})$ versus $1/T$ plots. All calculated ΔH and ΔS values are given in Table 4. For all the compounds, ΔS_D is large and positive, as

Table 4
Thermodynamic data for Group 13 halide complexes of 9-fluorenone[a]

Compound	K_{eq} at 298 K (mol dm^{-3})	ΔH (kJ mol^{-1})	ΔS (J K^{-1} mol^{-1})	ΔG at 298 K (kJ mol^{-1})
BCl_3(9-fluorenone) (**1**)	$2.78(1) \times 10^{-6}$	125(1)	313(2)	32(2)
$AlCl_3$(9-fluorenone)	$6.34(3) \times 10^{-4}$	85.8(5)	227(3)	18(1)
$AlBr_3$(9-fluorenone) (**2**)	$5.68(5) \times 10^{-4}$	92.4(9)	248(3)	19(1)
$GaCl_3$(9-fluorenone) (**5**)	$2.117(5) \times 10^{-3}$	78.8(5)	214(2)	15(1)
$GaBr_3$(9-fluorenone) (**6**)	$4.07(7) \times 10^{-3}$	152.0(3)	465(7)	13(2)

[a] Error is given in parentheses.

would be expected from a dissociative process. However, a direct comparison of the numbers is difficult due to potential complications with dimerization of the free MX_3.

2.3. *Is there a simple parameter for measuring Lewis acidity?*

Before resorting to techniques such as principle component analysis using a number of spectroscopic and structural parameters we have investigated if there is a consistent trend in the various parameters that will allow for easy prediction of Lewis acidity by a single measurement. In this regard, we have correlated the results for the five structurally characterized compounds MX_3 ($M = B$, $X = Cl$; $M = Al$, $X = Cl$, Br; $M = Ga$, $X = Cl$, Br). Table 5 provides a summary of the relative trends as measured by each technique. Those compounds where additional spectroscopic data is available are also discussed in context. It is readily apparent from Table 5 that there is some disagreement between methods.

The shift in the carbonyl IR stretching frequency ($\Delta\nu_{C=O}$) for MX_3(9-fluorenone) follows the same trends reported by Lappert [1]. If the largest shift in the stretching frequency is associated with increased Lewis acidity of MX_3, then for the chlorides the order follows $B > Ga > Al$. For AlX_3 the order of $Br > Cl$ also follows the trend reported previously for Al and In [1]. Interestingly, the relative order for GaX_3 is the reverse (i.e. $Cl > Br$). This is the same as Lappert reported for boron [1], suggesting that the trend reverses between boron and aluminum, aluminum and gallium and then gallium and indium. However, we note that inclusion of MI_3 (see data in Table 1) does follow the appropriate trends, i.e. $AlI_3 \approx AlBr_3 > AlCl_3$ and $GaCl_3 > GaBr_3 > GaI_3$. The advantage with the IR parameter is that isolation of the compound is not required, and it should provide a suitable measurement for 1:2 complexes. Thus, IR would place $ZrCl_4$ between BCl_3 and $AlBr_3$, while $SnCl_4$ would be comparable to $GaCl_3$. Furthermore, the similarity of GaI_3 and $MgCl_2$ for which the 1:2 complexes are common [34], suggests that GaI_3(9-fluorenone)$_2$ is the sole complex formed.

Table 5
Summary of spectroscopic and structural trends for MX_3(9-fluorenone).

Technique	Parameter [a]	Trend
IR	$\Delta\nu_{C=O}$	$BCl_3 > AlBr_3 > GaCl_3 > GaBr_3 > AlCl_3$
UV–vis	$\Delta\lambda_{max}$	$BCl_3 > AlBr_3 > AlCl_3 > GaBr_3 > GaCl_3$
^{13}C-NMR	$\Delta\delta_{C=O}$	$GaCl_3 > GaBr_3 \approx AlCl_3 > AlBr_3 > BCl_3$
^{1}H-NMR	K_{eq} at 298 K	$BCl_3 > AlBr_3 > AlCl_3 > GaCl_3 > GaBr_3$
	ΔH	$GaBr_3 > BCl_3 > AlBr_3 > AlCl_3 > GaCl_3$
	ΔG	$BCl_3 > AlBr_3 > AlCl_3 > GaCl_3 > GaBr_3$
XRD	O(1)–C(9)	$AlBr_3 > AlCl_3 > BCl_3 > GaBr_3 > GaCl_3$
	Σ(X–M–X)	$AlBr_3 > AlCl_3 > BCl_3 > GaCl_3 > GaBr_3$
	$\Delta_{O,X}$	$AlBr_3 > AlCl_3 > BCl_3 > GaCl_3 > GaBr_3$

[a] See text for definitions.

The shift of the λ_{max} for MX_3(9-fluorenone) as compared to the free ligand ($\Delta\lambda_{max}$) follows $B > Ga > Al$; a different trend to that obtained from IR spectroscopy. Our data is in concert with the theoretically calculated values for π* with regard $BCl_3 > AlBr_3 > AlCl_3$ [16,17]. These π* values reported by Lazlo and Teston were not dependent on the transition, but rather the absolute energy of the level in eV. We have not determined the nature of the observed absorption, and if it is associated with a $M{-}X_\sigma \rightarrow L\ \pi^*$ transition, as is commonly observed for intensely colored Group 13 compounds [35,36], then the relative ordering is going to depend on the relative energies of the $M{-}X_\sigma$ orbitals.

We have previously suggested that an increased downfield shift in the ^{13}C-NMR signal for the *C*=O carbon of an organic carbonyl as compared to the free ligand ($\Delta\delta_{C=O}$), correlates with the activation of the carbonyl towards nucleophilic attack [19]. Furthermore, it would be assumed that the larger shifts are associated with stronger Lewis acid–base interactions. As may be seen from Table 5, the trend obtained from ^{13}C-NMR ($\Delta\delta_{C=O}$) is essentially the reverse of the order found by any other parameter. There is even an almost inverse relationship between $\Delta\delta_{C=O}$ and ΔG, suggesting that while our proposal that $\Delta\delta_{C=O}$ can be correlated to reactivity, it clearly is not related to the strength of the Lewis acid–base interaction in MX_3(9-fluorenone). We note that ^{13}C-NMR shifts may be affected by paramagnetic shielding of excited states, which may result in trends opposite to sigma inductive effects. Presumably a similar effect is occurring in this series.

Solution dissociation enthalpies have been assumed to represent the BDE for simple Lewis acid base complexes, and in the absence of potential dimerization (Eq. (2)) they may be appropriate [10].

$$2MX_3 \overset{K_{eq}}{\rightleftharpoons} [X_2M(\mu\text{-}X)]_2 \qquad (2)$$

However, in the present study it is clear that ΔH is not representative of Lewis acid strength. For example, the ΔH for $GaBr_3$ is the largest, but it has the highest dissociation constant at 298 K (see Table 4). This would suggest that the entropy term is very important in defining the extent of a Lewis acid–base interaction in solution. In contrast, the trend found for ΔG more closely matches that expected. Although ΔH defines the energy of the reaction between the Lewis acid and base, it does not take into account the extent of reaction at a given temperature. Thus, if the Lewis acid catalyzes a reaction that does not proceed in the absence of the Lewis acid, the 'level of activation' rather than the 'extent of reaction' may be more important. In contrast, if the reaction under consideration occurs in the absence of a Lewis acid, but the presence of the Lewis acid changes the site selectivity (e.g. alkylation of a 1,3-enone at the 2 or 4 positions) then the extent of reaction will be more important. In this regard we propose that the value of K_{eq} taken at a defined temperature (e.g. 298 K) may be a more useful parameter to determine the suitability of a Lewis acid as a catalyst. Unfortunately, neither of the simpler spectroscopic measurements (IR and UV) provide a positive correlation with either K_{eq} or ΔG.

Structural parameters are commonly employed in discussion of the strength of a Lewis acid interaction. As would be expected the M–O distance in MX_3(9-fluorenone) are dependent on the ionic radii of the Group 13 element (Fig. 4). In fact, the experimental values for M–O and M–X are predicted with reasonable accuracy from the sum of the ionic radii (Fig. 5). By comparison the use of the covalent radii overestimates the M–O distances and underestimates the M–X distances (see Fig. 5). Thus, the M–O distance cannot be used as a measure of relative Lewis acidity between complexes of dissimilar metals, however, based upon the relative M–O distances the trends $AlBr_3 > AlCl_3$ and $GaCl_3 > GaBr_3$ would be expected, which is in line with the IR data. The C=O bond length should provide a comparison between complexes with different metals, and also should correlate with IR data is the change in the $\nu_{C=O}$ is associated with weakening of the bond (rather than changes in the reduced mass). Despite the presence of a trend (see Table 5), the values are sufficiently close and the esds large enough, that no real comparison may be made.

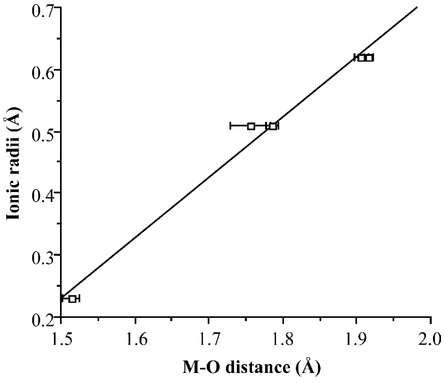

Fig. 4. Plot showing the relationship between M–O bond length in the complexes MX_3(9-fluorenone) (M = B, Al, Ga; X = Cl, Br) and the ionic radii for M ($R = 0.986$).

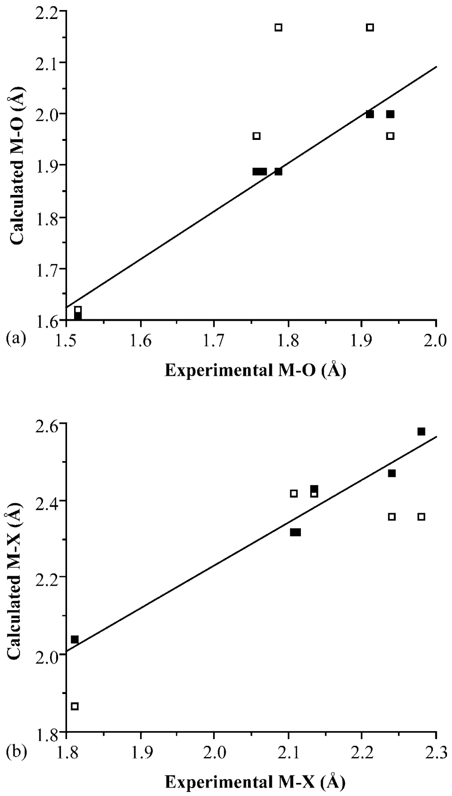

Fig. 5. Plot showing the relationship between experimental (a) M–O and M–X bond lengths in the complexes MX_3(9-fluorenone) (M = B, Al, Ga; X = Cl, Br) and the sum of the ionic radii (■) and covalent radii (□) ($R_{(a)} = 0.979$; $R_{(a)} = 0.986$).

It is generally assumed that (in the absence of overwhelming steric effects) the stronger a Lewis acid–base interaction, the greater the geometry about the Lewis acid will be distorted from an ideal planar structure associated with a monomeric structure. An alternative approach to measure Lewis acidity is to study the distortions from ideal tetrahedral. Within a series for an individual metal the distortion from planar (Eq. 6), $AlBr_3 > AlCl_3$ and $GaCl_3 > GaBr_3$, both of which are consistent with IR data. However, as may be seen from Fig. 6, the deviation from planarity is closely related to the M–O distance. This would suggest that intra-

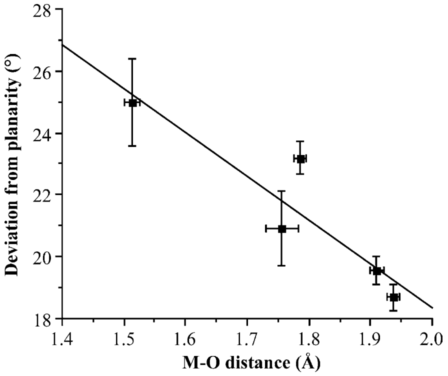

Fig. 6. Plot of the deviation from planarity of the Group 13 element in MX_3(9-fluorenone) (M = B, Al, Ga; X = Cl, Br) as a function of the M–O bond length (R −0.851).

molecular repulsion is the controlling factor with regard to the geometry about the Group 13 center. We have previously shown that such a relationship is predominant in the phosphine complexes of $AlMe_3$ [4].

It has been noted that a consideration of the covalent radii and bond lengths reported for organic molecules would predict a metal alkoxide or aryloxide σ-bond length to be 0.10–0.15 Å shorter than a metal–alkyl bond. Therefore, the parameter $\Delta_{O,C}$ was proposed (Eq. (3)) as a qualitative probe for possible π-bonding between aryloxide, oxygen atoms, and electron-deficient metal centers [37].

$$\Delta_{O,X} = d(M–O) - d(M–X) \quad (3)$$

Given the clear ionic character of the bonding in MX_3(9-fluorenone), we can propose a similar parameter, $\Delta_{O,X}$, using the ideal M–O and M–X bond lengths (see Figure 5). The difference between the $\Delta_{O,X}$ (Eq. 3) value calculated for each M–X combination and the experimentally determined M–O and M–X bond lengths allows for a measure of the shortening of the M–O bond over that expected. As is shown in Table 5, this order follows that of Σ(X–M–X). In addition, it suggest the trends $AlBr_3 > AlCl_3$ and $GaCl_3 > GaBr_3$, the order of which is observed from IR spectroscopy.

Based on all the forgoing, it is clear that none of the spectroscopic or structural parameters studied herein provides a consistent prediction of Lewis acid strength. However, we propose that the parameters investigated above, in combination with a series of kinetic parameters, would provide the ideal basis for a principle component analysis of measured Lewis acid properties. In conclusion, it appears that unlike Bronsted acidity, Lewis acidity (pK_a) does not have a simple parameter that will allow for comparison of a range of compounds.

3. Experimental

Mass spectra were obtained on a Finnigan MAT 95 mass spectrometer operating with an electron beam energy of 70 eV for EI mass spectra. IR spectra (4000–400 cm^{-1}) were obtained using a Nicolet 760 FT-IR infrared spectrometer. NMR spectra were obtained on Bruker Avance 200, 400, and 500 spectrometers using (unless otherwise stated) d_6-benzene solutions. Chemical shifts are reported relative to internal solvent resonances (^1H and ^{13}C), and external $[Al(H_2O)_6]^{3+}$ (^{27}Al). $GaCl_3$ was obtained from Strem Chemicals. All other Lewis acids, as well as 9-fluorenone, were obtained from Aldrich. The Lewis acids were used without further purification; 9-fluorenone was recrystallized from $C_6H_5CH_3$ prior to use.

3.1. *BCl_3(9-fluorenone) (**1**)*

BCl_3 (0.586 g, 5.0 mmol) in *o*-xylene (50 ml) was added to 9-fluorenone (0.901 g, 5.0 mmol) in *o*-xylene (25 ml), resulting in a dark red solution. The reaction mixture was allowed to stir at room temperature (r.t.) for 2 h, then was cooled at −24 °C for several days, resulting in the formation of dark red crystalline blocks. Yield: 65%. M.p.: 150 °C (dec.). MS (EI, %): *m/z* 180 ($C_{13}H_8O$, 100). IR (cm^{-1}): 1611 (m), 1603 (s), 1583 (m), 1558 (s), 1310 (s), 1234 (w), 1206 (m), 1090 (w), 936 (m), 813 (s), 786 (m), 734 (s), 694 (m), 669 (w), 642 (w), 562 (m). ^{1}H-NMR: δ 7.72 [2H, d, J(H–H) = 7.5 Hz, 1-C*H*], 6.56 [2H, dt, J(H–H) = 7.5 Hz, J(H–H) = 1.1 Hz, 3-C*H*], 6.31 [2H, dt, J(H–H) = 7.6 Hz, J(H–H) = 0.9 Hz, 2-C*H*], 6.25 [2H, d, J(H–H) = 7.3 Hz, 4-C*H*]. ^{13}C-NMR: δ 200.2 (9-*C*), 146.7 (10-*C*), 139.6 (3-*C*), 133.2 (11-*C*), 130.2 (2-*C*), 126.0 (1-*C*), 121.5 (4-*C*).

3.2. *$AlCl_3$(9-fluorenone)*

Prepared as previously described in the literature [25]. Yield: 75%. M.p.: 206 °C (dec.). MS (EI, %): *m/z* 277 ([M^+ −Cl], 10), 241 ([M^+ −Cl−H], 10), 180 ($C_{13}H_8O$, 100). IR (cm^{-1}): 1637 (s), 1602 (s), 1573 (s), 1313 (s), 1236 (w), 1210 (m), 1190 (w), 1163 (w), 1097 (m), 1007 (m), 1003 (w), 960 (w), 928 (m), 815 (w), 799 (m), 734 (s), 627 (w), 652 (m), 633 (s). ^{1}H-NMR: δ 7.49 [2H, dd, J(H–H) = 7.5 Hz, J(H–H) = 0.4 Hz, 1-C*H*], 6.86 [2H, t, J(H–H) = 7.5 Hz, 3-C*H*], 6.79 [2H, d, J(H–H) = 6.8 Hz, 4-C*H*], 6.65 [2H, t, J(H–H) = 7.5 Hz, 2-C*H*]. ^{13}C-NMR: δ 197.2 (9-*C*), 145.6 (10-*C*), 136.9 (3-*C*), 134.2 (11-*C*), 130.6 (2-*C*), 129.8 (1-*C*), 121.1 (4-*C*). ^{27}Al-NMR (C_7H_8–C_6D_6): δ 93 ($W_{1/2}$ = 1800 Hz).

3.3. *$AlBr_3$(9-fluorenone) (**2**)*

Toluene (30 ml) was added to 9-fluorenone (0.169 g, 0.94 mmol) and an excess of $AlBr_3$ (0.500 g, 1.88 mmol) at r.t. The resulting red solution was allowed to stir at r.t. for 3 h. The solution was then filtered and cooled to −24 °C. Dark red crystalline needles formed overnight. Yield: 80%. M.p.: 179 °C (dec.). MS (EI, %): *m*/*z* 444 ([M$^+$], 5), 365 ([M$^+$ −Br], 10), 285 ([M$^+$ −Br−H], 10), 265 ($AlBr_3$, 5), 185 ($AlBr_2$, 10), 180 ($C_{13}H_8O$, 100), 79 (Br, 5). IR (cm^{-1}): 1640 (s), 1603 (s), 1576 (s), 1312 (m), 1231 (w), 1207 (w), 1093 (m), 1030 (w), 1001 (w), 963 (w), 926 (w), 895 (w), 802 (m), 728 (s), 694 (w), 641 (m). ^{1}H-NMR: δ 7.38 [2H, d, *J*(H−H) = 7.4 Hz, 1-C*H*], 6.54 [2H, dt, *J*(H−H) = 7.5 Hz, *J*(H−H) = 0.8 Hz, 2-C*H*], 6.22 [2H, t, 7.6 Hz, 3-C*H*], 6.20 [2H, d, *J*(H−H) = 7.3 Hz, 4-C*H*].^{13}C-NMR: 204.5 (9-*C*), 147.3 (10-*C*), 141.7 (3-*C*), 132.7 (11-*C*), 132.2 (2-*C*), 130.7 (1-*C*), 122.3 (4-*C*). ^{27}Al-NMR (C_7H_8–C_6D_6): δ 82 ($W_{1/2}$ = 3800 Hz).

3.4. *AlBr$_3$(9-fluorenone)$_2$ (**3**)*

Prepared in the same manner as compound **2**, but using 9-fluorenone (0.169 g, 0.94 mmol) and $AlBr_3$ (0.250 g, 0.94 mmol). Upon cooling, a mixture of compounds **2** and **3** formed. Yield: 25%. M.p.: 179 °C (dec.). MS (EI, %): *m*/*z* 444 ([M$^+$], 5), 365 ([M$^+$ −Br], 10), 285 ([M$^+$ −Br−H], 10), 265 ($AlBr_3$, 5), 185 ($AlBr_2$, 10), 180 ($C_{13}H_8O$, 100), 79 (Br, 5). IR (cm^{-1}): 1668 (s), 1607 (s), 1590 (s), 1307 (s), 1205 (s), 1158 (w), 1089 (m), 962 (w), 920 (s), 892 (m), 813 (m), 729 (s), 694 (m), 671 (m), 642 (m), 604 (s). ^{1}H-NMR: δ 7.47 [2H, d, *J*(H−H) = 7.4 Hz, 1-C*H*], 6.79 [2H, t, *J*(H−H) = 7.5 Hz, 2-C*H*], 6.65 [2H, d, J(H−H) = 7.3 Hz, 4-C*H*], 6.55 [2H, *J*(H−H) = 7.5 Hz, 3-C*H*]. ^{13}C-NMR: δ 197.9 (9-C), 145.8 (10-*C*), 137.5 (3-*C*), 134.0 (11-*C*), 129.9 (2-*C*), 127.7 (1-*C*), 121.3 (4-*C*). ^{27}Al-NMR (C_7H_8–C_6D_6): δ 82 ($W_{1/2}$ = 3800 Hz).

3.5. *AlI$_3$(9-fluorenone)$_2$ (**4**)*

Prepared in the same manner as **2**, but using 9-fluorenone (44 mg, 0.25 mmol) and AlI_3 (0.101 g, 0.25 mmol). AlI_3 is light-sensitive, so, though no decomposition was observed when leaving **4** exposed to light, the reaction vessel was protected from light by aluminum foil. Yield: 55%. M.p.: 174 °C (dec.). MS (EI, %): *m*/*z* 588 ([M$^+$], 5), 461 ([M$^+$ −I], 100), 333 ([M$^+$ −2 I−H], 30), 281 (AlI_2, 35), 207 ([M$^+$ −3 I], 10), 180 ($C_{13}H_8O$, 40), 152 ($C_{13}H_8O$−CO, 50), 151 ($C_{13}H_8O$−CO−H, 100). IR (cm^{-1}): 1634 (m), 1601 (m), 1572 (m), 1311 (w), 729 (s).

3.6. *GaCl$_3$(9-fluorenone) (**5**)*

Prepared in the same manner as compound **1**, but using $GaCl_3$ (0.489 g, 2.77 mmol). Yield: 85%. M.p.: 171 °C (dec.). MS (EI, %): *m*/*z* 180 ($C_{13}H_8O$, 100), 152 ($C_{12}H_8$, 25), 76 (C_6H_4, 10). IR (cm^{-1}): 1635 (s), 1603 (s), 1573 (s), 1310 (s), 1237 (w), 1206 (m), 1188 (w), 1159 (w), 1098 (m), 1090 (m), 927 (m), 734 (s). ^{1}H-NMR: δ 7.38 [2H, d, *J*(H−H) = 7.4 Hz, 1-C*H*], 6.63 [2H, dt, *J*(H−H) = 7.2 Hz, *J*(H−H) = 0.8 Hz, 3-C*H*], 6.33 [2H, t, *J*(H−H) = 7.9 Hz, 2-C*H*], 6.32 [2H, d, *J*(H−H) = 7.7 Hz, 4-C*H*]. ^{13}C-NMR: δ 203.6 (9-*C*), 146.6 (10-*C*), 139.5 (3-*C*), 132.5 (11-*C*), 131.7 (2-*C*), 128.2 (1-*C*), 121.5 (4-*C*).

3.7. *GaBr$_3$(9-fluorenone) (**6**)*

Prepared in the same manner as compound **1**, but using 9-fluorenone (0.146 g, 0.810 mmol) and $GaBr_3$ (0.250 g, 0.810 mmol). Yield: 80%. M.p.: 147 °C (dec.). MS (EI, %): *m*/*z* 306 ($GaBr_3$, 15), 227 ($GaBr_2$, 35), 180 ($C_{13}H_8O$, 100), 152 ($C_{12}H_8$, 35). IR (cm^{-1}): 1636 (m), 1605 (m), 1569 (m), 1495 (w), 1308 (m), 1204 (w), 1096 (w), 1030 (w), 956 (w), 924 (w), 812 (m), 783 (w), 727 (s), 694 (m), 670 (w), 648 (w), 602 (w), 439 (m). ^{1}H-NMR: 7.51 [2H, d, *J*(H−H) = 7.5 Hz, 1-C*H*], 6.59 [2H, dt, *J*(H−H) = 7.5 Hz, *J*(H−H) = 1.0 Hz, 3-C*H*], 6.34 [2H, dt, *J*(H−H) = 7.6 Hz, *J*(H−H) = 0.8 Hz, 2-C*H*], 6.30 [2H, d, *J*(H−H) = 7.4 Hz, 4-C*H*]. ^{13}C-NMR: 204.0 (9-*C*), 146.5 (10-*C*), 139.5 (3-*C*), 138.2 (11-*C*), 130.9 (2-*C*), 129.7 (1-*C*), 121.5 (4-*C*).

3.8. *GaI$_3$(9-fluorenone)$_2$ (7)*

Prepared in the same manner as **1**, but with 9-fluorenone (40 mg, 0.22 mmol) and GaI_3 (0.2 g, 0.444 mmol). Yield: 70%. M.p.: 156 °C (dec.). MS (EI, %): *m*/*z* 450 (GaI_3, 25), 323 (GaI_2, 30), 198, 180 ($C_{13}H_8O$, 100), 152 ($C_{13}H_8O$−CO, 40), 127 (I, 10). IR (cm^{-1}): 1652 (w), 1603 (w), 1558 (w), 1395 (m), 1153 (w), 919 (w), 728 (m). ^{1}H-NMR: 7.62 [2H, d, *J*(H−H) = 7.4 Hz, 1-C*H*], 6.58 [2H, dt, *J*(H−H) = 7.5 Hz, *J*(H−H) = 1.0 Hz, 2-C*H*], 6.36 [2H, dt, *J*(H−H) = 7.6 Hz, *J*(H−H) = 0.8 Hz, 3-C*H*], 6.29 [2H, d, *J*(H−H) = 7.4 Hz, 4-C*H*]. ^{13}C-NMR: 205.2 (9-*C*), 146.8 (10-*C*), 140.8 (3-*C*), 132.3 (11-*C*), 131.3 (2-*C*), 130.4 (1-*C*), 122.2 (4-*C*).

3.9. *MgCl$_2$(9-fluorenone)$_n$ (**8**)*

Sample prepared for IR spectroscopic characterization by grinding 9-fluorenone (10 mg, 55 μmol) and an excess of $MgCl_2$ (50 mg, 0.53 mmol) into a very fine mixture. IR (cm^{-1}): 1653 (m), 1611 (s), 1297 (m), 1190 (m), 1149 (s), 1096 (m), 949 (w), 916 (m), 811 (w), 782 (w), 735 (s), (668 (m).

3.10. *HgCl$_2$(9-fluorenone)$_n$ (**9**)*

Sample prepared for IR spectroscopic characterization in the same manner as **8**, but using $HgCl_2$ (50 mg, 0.18 mmol). IR (cm^{-1}): 1697 (s), 1612 (m), 1599 (m), 1300 (m), 735 (s), 728 (s).

3.11. *$ZrCl_4$(9-fluorenone)$_n$* (**10**)

Sample prepared for IR spectroscopic characterization in the same manner as **8**, but using $ZrCl_4$ (50 mg, 0.21 mmol). As the two solids were ground together, a solid state reaction was observed, as evidenced by a color change from 9-fluorenone's yellow to brown. IR (cm^{-1}): 1632 (m), 1611 (m), 1601 (w), 1570 (m), 1299 (m), 1190 (m), 1150 (w), 916 (s), 735 (s).

3.12. *$SnCl_4$(9-fluorenone)$_2$* (**11**)

$SnCl_4$ (0.362 g, 1.39 mmol) was added by syringe to a $C_6H_5CH_3$ (60 ml) solution of 9-fluorenone (0.250 g, 1.39 mmol). The resulting orange–red solution was allowed to stir for several hours, then cooled to −24 °C. Red precipitate formed overnight. Yield: 75%. M.p.: 156 °C. MS (EI, %): *m/z* 225 ($SnCl_3$, 15), 180 ($C_{13}H_8O$, 100), 152 ($C_{13}H_8O{-}CO$, 35). IR (cm^{-1}): 1634 (s), 1607 (s), 1577 (s), 1310 (m), 1202 (m), 1097 (m), 1004 (w), 992 (w), 956 (m), 923 (m), 889 (m), 812 (m), 779 (m), 725 (s), 670 (m), 646 (w), 588 (s). ^{1}H-NMR: δ 7.65 [2H, dt, J(H–H) = 7.3 Hz, J(H–H) = 1.0 Hz, 1-C*H*], 6.92 (4H, m, 3- and 4-C*H*), 6.74 (2H, m, 2-C*H*). ^{13}C-NMR: 194.0 (9-*C*), 145.1 (10-*C*), 135.0 (3-*C*), 134.8 (11-*C*), 129.5 (2-*C*), 125.2 (1-*C*), 120.7 (4-*C*).

3.13. *VO(Cl)(9-fluorenone)$_2$(H_2O)(μ-O)($VOCl_2$)* (**12**)

Prepared in the same manner as **1.9**, but using hydrolyzed VCl_4 (0.268 g, 1.39 mmol) and 9-fluorenone (0.25 g, 1.39 mmol) Yield: 75%. M.p.: 194 °C (dec.). IR (cm^{-1}): 1657 (s), 1608 (m), 1587 (s), 1310 (m), 1207 (w), 1158 (w), 1011 (w), 923 (w), 850 (w), 811 (w), 730 (s), 667 (m).

3.14. *Crystallographic studies*

Crystals of **1**–**3**, **5**, **6**, and **12** were sealed in a glass capillary under Ar and mounted on the goniometer of a Bruker CCD SMART system, equipped with graphite monochromated Mo–K_α radiation (λ = 0.71073 Å) and corrected for Lp effects. Data collection and unit cell and space group determination were all carried out in the usual manner [36]. Pertinent details are given in

Table 6
Summary of X-ray diffraction data

Compound	BCl_3(9-fluorenone)·1/2(C_6H_5Me) (**1**)	$AlBr_3$(9-fluorenone)·1/2(C_6H_5Me) (**2**)	$AlBr_3$(9-fluorenone)$_2$ (**3**)	$GaCl_3$(9-fluorenone) (**5**)	$GaBr_3$(9-fluorenone)·1/2(C_6H_5Me) (**6**)	VO(Cl)(9-fluorenone)$_2$(H_2O)(μ-O)($VOCl_2$) (**12**)
Empirical formula	$C_{16.5}H_{12}BCl_3O$	$C_{16.5}H_{12}AlBr_3O$	$C_{26}H_{16}AlBr_3O_2$	$C_{13}H_9Cl_3GaO$	$C_{16.5}H_{12}Br_3GaO$	$C_{26}H_{18}Cl_3O_6V_2$
M_w	343.42	492.97	1254.20	357.27	535.71	634.63
Crystal system	Triclinic	Triclinic	Triclinic	Orthorhombic	Monoclinic	Triclinic
Space group	$P\bar{1}$	$P\bar{1}$	$P\bar{1}$	*Pbca*	$P2_1/n$	$P\bar{1}$
a (Å)	9.472(2)	9.645(2)	7.248(1)	9.210(2)	7.598(2)	9.806(2)
b (Å)	9.726(2)	10.020(2)	10.358(2)	17.153(3)	11.619(2)	10.259(2)
c (Å)	9.973(2)	10.546(2)	16.214(3)	17.531(4)	20.321(4)	14.098(3)
α (°)	79.92(3)	63.41(3)	86.47(3)			107.79(3)
β (°)	62.55(3)	80.91(3)	83.29(3)		96.71(3)	101.79(3)
γ (°)	88.01(3)	88.23(3)	71.03(3)			95.55(3)
V (Å^3)	801.6(3)	898.9(3)	1142.9(4)	2769.4(9)	1781.7(6)	1302.5(5)
Z	2	2	1	8	4	2
D_{calc} (g cm^{-3})	1.423	1.821	1.822	1.709	1.997	1.618
μ (cm^{-1})	0.57	6.78	5.36	2.55	8.27	1.07
2θ Range (°)	4.3–46.6	4.3–46.7	2.5–46.6	4.6–46.6	4.0–46.6	3.14–46.58
Reflections collected	3702	4156	5369	6468	7944	6035
Independent reflections	2284	2565	3296	1981	2568	3748
Reflections observed ($\lvert F_o\rvert > 4.0\sigma\lvert F_o\rvert$)	1830	1219	1802	1263	1616	1894
Weighting scheme	SHELXTL 0.0709, 0	SHELXTL 0.05, 0	SHELXTL, 0.04, 0	SHELXTL, 0.015, 0	SHELXTL, 0.04, 0	SHELXTL, 0.02, 0
R [a]	0.0399	0.0759	0.0630	0.0315	0.0383	0.0514
R_w [a]	0.1080	0.1617	0.1303	0.0543	0.0810	0.0835
Largest difference peak	0.34	0.72	0.95	0.34	0.48	0.44

[a] $R = \Sigma\ \lvert F_o - F_c\rvert / \Sigma\ F_o$; $wR = \{\Sigma\ [\{w(F_o^2 - F_c^2)^2\}/\{w(F_o^2)2\}]\}^{1/2}$.

Table 6. The structure was solved by direct methods (SHELXTL) [38], and the model was refined using full-matrix least-squares techniques. All hydrogen atoms were placed in calculated positions [$U_{iso} = 1.3U_{(C)}$; d(C–H) = 0.95 Å] for refinement. Rotational disorder of the BCl_3 unit in compound **1** was refined in a similar manner to that previously described for *tert*-butyl groups [39]. Compounds **1**, **2**, and **6** crystallize as $C_6H_5CH_3$ solvates. The $C_6H_5CH_3$ resides on a center of inversion so appropriate disorder models were used. In two cases (**2** and **6**) it was necessary to apply geometric restraints in order to achieve a sensible model. Refinement of positional and anisotropic thermal parameters led to convergence (Table 6).

4. Supplementary material

Crystallographic data for the structural analysis have been deposited with the Cambridge Crystallographic Data Centre, CCDC nos. 191812–191817 for compounds **1**, **2**, **3**, **5**, **6** and **12**, respectively. Copies of this information may be obtained free of charge from The Director, CCDC, 12 Union Road, Cambridge CB2 1EZ, UK (Fax: +44-1223-336033; or e-mail: deposit@ccdc.cam.ac.uk or www: http://www.ccdc.cam.ac.uk).

Acknowledgements

Financial support for this work is provided by the Robert A. Welch Foundation. The Bruker CCD Smart System Diffractometer was funded by the Robert A. Welch Foundation and the Bruker Avance 200 NMR spectrometer was purchased with funds from ONR Grant N00014-96-1-1146.

References

[1] M.F. Lappert, J. Chem. Soc. (1962) 542.

[2] C.A. Tolman, J. Am. Chem. Soc. 92 (1970) 2953.

[3] C.A. Tolman, Chem. Rev. 77 (1977) 616.

[4] A.R. Barron, J. Chem. Soc. Dalton Trans. (1988) 3047.

[5] D. Farcasiu, A. Ghenciu, Prog. NMR Spectrosc. 29 (1996) 129.

[6] G.A. Olah, G.K. Surya Prakash, J. Sommer, Superacids, Wiley-Interscience, New York, 1985, pp. 24–25.

[7] D. Farcasiu, M. Stan, J. Chem. Soc. Perkin Trans. (1998) 1219.

[8] R.J. Gillespie, J.S. Hartman, Can. J. Chem. 46 (1968) 2147.

[9] D.P.N. Satchell, R.S. Satchell, Chem. Rev. 69 (1969) 251.

[10] (a) M.B. Power, J.R. Nash, M.D. Healy, A.R. Barron, Organometallics 11 (1992) 1830;
(b) J.A. Francis, C.N. McMahon, S.G. Bott, A.R. Barron, Organometallics 18 (1999) 4399.

[11] S. Shambayti, W.E. Crowe, S.L. Schreiber, Angew. Chem. Int. Ed. Engl. 29 (1990) 256.

[12] (a) B.H. Davis, R.A. Keogh, S. Alerasool, D.J. Zalewski, D.E. Day, P.K. Doolin, J. Catal. 183 (1999) 45;
(b) G. Berhault, M. Lacroix, M. Breysse, F. Maugé, J.-C. Lavalley, H. Nie, L. Qu, J. Catal. 178 (1998) 555;
(c) C. Morterra, G. Cerrato, V. Bolis, S. Di Ciero, M. Signoretto, J. Chem. Soc. Faraday Trans. 93 (1997) 1179;
(d) G. Catana, D. Baetens, T. Nommaerts, R.A. Schoonheydt, B.M. Weckhuysen, J. Phys. Chem. Sect. B 105 (2001) 4904.

[13] B. Hu, I.D. Gay, J. Phys. Chem. Sect. B 105 (2001) 217.

[14] M.F. Lappert, J. Chem. Soc. (1961) 817.

[15] R.F. Childs, D.L. Mulholland, A. Nixon, Can. J. Chem. 60 (1982) 801.

[16] P. Laszlo, M. Teston, J. Am. Chem. Soc. 112 (1990) 8750.

[17] P. Laszlo, M. Teston-Henry, Tetrahedron Lett. 32 (1991) 3837.

[18] R. Carlson, T. Lundstedt, A. Nordahl, M. Prochazka, Acta Chem. Scand. B40 (1986) 522.

[19] M.B. Power, S.G. Bott, J.L. Atwood, A.R. Barron, J. Am. Chem. Soc. 112 (1990) 3446.

[20] G.D. Smith, P.E. Fanwick, I.P. Rothwell, Inorg. Chem. 29 (1990) 3221.

[21] M.B. Power, S.G. Bott, D.L. Clark, J.L. Atwood, A.R. Barron, Organometallics 9 (1990) 3086.

[22] M. Akakura, H. Yamamoto, S.G. Bott, A.R. Barron, Polyhedron 16 (1997) 4389.

[23] (a) V. Sharma, M. Simard, J.D. Wuest, J. Am. Chem. Soc. 114 (1992) 7931;
(b) G. Quinkert, H. Becker, M. Del Grosso, G. Dambacher, J.W. Bats, G. Dürner, Tetrahedron Lett. 34 (1993) 6885;
(c) A.P. Shreve, R. Mulhaupt, W. Fultz, J. Calabrese, W. Robbins, S.D. Ittel, Organometallics 7 (1988) 409;
(d) G. Sartori, F. Bigi, X. Tao, C. Porta, R. Maggi, G. Predieri, M. Lanfranchi, M.A. Pellinghelli, J. Org. Chem. 60 (1995) 6588;
(e) B. Chevrier, J.-M. Le Carpentier, R. Weiss, Acta Crystallogr. Sect. B 28 (1972) 2659;
(f) A. Bittner, D. Mannig, H. Noth, Z. Naturforsch. Tiel. B 41 (1986) 587;
(g) S.E. Rasmussen, N.C. Broch, Acta Chem. Scand. 20 (1966) 1351;
(h) J. Utko, M. Wróblewska, T. Lis, P. Sobota, J. Organomet. Chem. 447 (1993) 159;
(i) F. Bigi, G. Sartori, R. Maggi, C. Valerio-Papa, E. Marzi, M. Lanfranchi, M.A. Pellinghelli, J. Chem. Soc. Perkin Trans. 1 (1996) 1815;
(j) P. Sobota, S. Szafert, T. Glowiak, J. Organomet. Chem. 526 (1996) 329.

[24] (a) R.L. Beddoes, D. Collison, F.E. Mabbs, J. Temperley, Acta Crystallogr. Sect. C 47 (1991) 58;
(b) S. Jin, V. McKee, M. Nieuwenhuyzen, W.T. Robinson, C.J. Wilkins, J. Chem. Soc. Dalton Trans. (1993) 3111.

[25] D.L. Boucher, M.A. Brown, B.R. McGarvey, D.G. Tuck, J. Chem. Soc. Dalton Trans. (1999) 3445.

[26] H. Kuroda, T.L. Kunii, Theor. Chim. Acta 9 (1967) 51.

[27] H.R. Luss, D.L. Smith, Acta Crystallogr. Sect. B 28 (1972) 884.

[28] See, for example: (a) F. Avecilla, C.F.G.C. Geraldes, M.M.C.A. Castro, Eur. J. Inorg. Chem. (2001) 3135;
(b) Y. Sun, M. Melchior, D.A. Summers, R.C. Thompson, S.J. Rettig, C. Orvig, Inorg. Chem. 37 (1998) 3119;
(c) K. Isobe, S.I. Ooi, Y. Nakamura, S. Kawaguchi, H. Kuroya, Chem. Lett. (1975) 35;
(d) C.R. Cornman, J. Kampf, M.S. Lah, V.L. Pecoraro, Inorg. Chem. 31 (1992) 2035;
(e) X. Li, M.S. Lah, V.L. Pecoraro, Inorg. Chem. 27 (1988) 4657;
(f) M.R. Caira, J.M. Haigh, L.R. Nassimbeni, J. Inorg. Nucl. Chem. 24 (1972) 3171.

[29] (a) H.C. Brown, N. Davidson, J. Am. Chem. Soc. 64 (1942) 316;
(b) G. Bahr, G.E. Muller, Chem. Ber. 88 (1955) 251;
(c) E. Bonitz, Chem. Ber. 88 (1955) 742;
(d) W.L. Everson, E.M. Ramirez, Anal. Chem. 37 (1965) 806;
(e) C.H. Henrickson, D.P. Eyman, Inorg. Chem. 6 (1967) 1461;
(f) C.H. Henrickson, K.M. Nykerk, D.P. Eyman, Inorg. Chem. 7

(1968) 1028;
(g) C.H. Henrickson, D. Duffy, D.P. Eyman, Inorg. Chem. 7 (1968) 1047;
(h) Z.h. S. Galuashvili, I.P. Romm, E.N. Gur'yanova, N.N. Korneev, K.A. Kocheshkov, Bull. Acad. Sci. USSR Div. Chem. Sci. 24 (1975) 2598.

[30] M.D. Healy, J.W. Ziller, A.R. Barron, Organometallics 10 (1991) 597.

[31] (a) R. Amunugama, M.T. Rodgers, J. Phys. Chem. Sect. A 105 (2001) 9883;
(b) M. Czerw, A.S. Goldman, K. Krogh-Jesperson, Inorg. Chem. 39 (2000) 363.

[32] (a) M.B. Smith, J. Phys. Chem. 71 (1967) 364;
(b) M.B. Smith, J. Organomet. Chem. 22 (1970) 273;
(c) M.B. Smith, J. Organomet. Chem. 46 (1972) 31;
(d) M.B. Smith, J. Organomet. Chem. 46 (1972) 211;
(e) M.B. Smith, J. Organomet. Chem. 70 (1974) 13.

[33] J.A.G. Drake, D.W. Jones, Spectrochim. Acta 36A (1980) 23.

[34] (a) H. Kageyama, K. Miki, Y. Kai, N. Kasai, Y. Okamoto, H. Yuki, Bull. Chem. Soc. Jpn. 56 (1983) 2411;
(b) X. Shijing, Q. Minxie, Z. Naijue, T. Youqi, Sci. Sin. Ser. B (Engl. Ed.) 30 (1987) 1247;
(c) C. Dohmeier, D. Loos, C. Robl, H. Schnockel, D. Fenske, J. Organomet. Chem. 448 (1993) 5;
(d) D.E. Hibbs, C. Jones, A.F. Richards, J. Chem. Soc. Dalton Trans. (1999) 3531.

[35] (a) J. Beumgarten, C. Bessenbacher, W. Kaim, T. Stahl, J. Am. Chem. Soc. 111 (1989) 2126;
(b) D.L. Lichtenberger, R.H. Hogan, M.D. Healy, A.R. Barron, Organometallics 10 (1991) 609.

[36] M.R. Mason, J.M. Smith, S.G. Bott, A.R. Barron, J. Am. Chem. Soc. 115 (1993) 4971.

[37] G.D. Smith, P.E. Fanwick, I.P. Rothwell, Inorg. Chem. 29 (1990) 3221.

[38] G.M. Sheldrick, Acta Crystallogr. Sect. A 46 (1990) 467.

[39] C.J. Harlan, E.G. Gillan, S.G. Bott, A.R. Barron, Organometallics 15 (1996) 5479.